Composites: Part A 175 (2023) 107744

Contents lists available at ScienceDirect

Composites Part A

journal homepage: www.elsevier.com/locate/compositesa

A punching process to join metal sheets and fibre reinforced polymer composites by mechanical interlocking

Núria Latorre [a,b,*], Daniel Casellas [a,c], Josep Costa [b]

[a] Eurecat, Centre Tecnològic de Catalunya, Unit of Polymeric and Composite Processes, Av. Universitat Autònoma 23, 08290 Cerdanyola del Vallès, Spain
[b] AMADE, Polytechnic School, University of Girona, Av. Universitat de Girona, 4, 17003 Girona, Spain
[c] Luleå University of Technology, Division of Solid Mechanics, 97187 Luleå, Sweden

ARTICLE INFO

Keywords:
Hybrid joint
Punching
Metal
CFRP

ABSTRACT

In the multi-material lightweight design of structural components for the automotive industry, the joint between different materials plays a significant role in reducing vehicle weight without compromising performance or safety. Conventional technologies to mechanically join metals and carbon fibre reinforced polymers result in either drilling a hole in the composite material or increasing the weight of the part because of the fasteners employed. This work presents a new, simple, cost-efficient and non-weight penalizing mechanical joining technology for metal sheets and fibre reinforced polymer prepregs. It consists of a single-step punching process where the metallic sheet is completely perforated, but the prepreg is not. The punch pushes the carbon fibres through the hole in the metal sheet with no or minimal fibre breakage, generating a mechanical interlock which, in turn, increases the shear strength and absorbed energy of the co-cured joint.

1. Introduction

Growing concern over fuel consumption and pollutant emissions is currently driving transport industry efforts towards reducing vehicle weight. Known as lightweighting, this decrease in weight lowers fuel-powered vehicle CO_2 emissions and increases the driving range of electric vehicles.

High-strength materials, such as advanced high-strength steels, aluminium alloys, or Fibre Reinforced Polymers (FRP) have been successfully used not only to reduce weight, but also to provide higher mechanical performance and increase passenger safety.

Therefore, the next step in vehicle lightweighting strategy is to use Multi-Material Design (MMD) for structural components to affordably meet mechanical and safety requirements and high production demands. MMD encourages employing the most suitable material for each part produced, tailoring component properties to balance maximum weight reduction, processability, performance and durability, to minimum costs [1]. There is, therefore, increased interest in MMD from the automotive industry, especially in the combination of light-weight metals, such as aluminium alloys, with Carbon Fibre Reinforced Polymers (CFRP).

Keeping this in mind, the joint between these dissimilar materials is usually the weakest point of the structure and determines its structural efficiency [2]. Traditional joining strategies for metal-FRP multi-material structures include mechanical fastening, adhesive bonding, hybrid mechanical-adhesive bonding and welding [3–5].

Mechanical fastening strategies generate a mechanical interlock between two materials, with their main advantages being its low cost, simple processing, easy maintenance and the fact that they are not sensitive to the working environment [4,6].

Conventional mechanical joining strategies for metals and CFRP include bolted joining [4–7], Self-Piercing Rivets (SPR) [8–11] and mechanical clinching [12–15]. However, these conventional methodologies either increase the weight of the structure with the incorporation of fasteners or entail drilling a hole in the composite. This perforation can cause damage such as delamination or fibre breakage, thus reducing the load bearing capacity of the structure [15,16].

To overcome such drawbacks, alternative mechanical interlocking procedures have also been proposed, such as pin joints [17–22] or loop joints [23], among other joining methodologies. However, all involve highly complex processing [24], which hinders their industrial application for high volume markets such as the automotive one.

Modifications to conventional mechanical joints have also been developed, such as incorporating bonded metallic inserts in the

* Corresponding author at: Eurecat, Centre Tecnològic de Catalunya, Av. Universitat Autònoma 23, 08290 Cerdanyola del Vallès, Spain.
E-mail addresses: nuria.latorre@eurecat.org (N. Latorre), daniel.casellas@eurecat.org (D. Casellas), josep.costa@udg.edu (J. Costa).

https://doi.org/10.1016/j.compositesa.2023.107744
Received 6 March 2023; Received in revised form 24 July 2023; Accepted 13 August 2023
Available online 14 August 2023

composite to reduce the stress concentration factors at the hole in the composite [25]. Other authors proposed steering the fibres onto the tacky prepreg to match the load path to improve the stiffness and strength of the bolted joint [26]. A post-curing SPR method to join CFRP and aluminium alloy sheets has also been proposed to reduce the damage generated in the composite material. In this process, the uncured prepreg and aluminium alloy are riveted together before being cured in an autoclave [11]. Conventional clinching has also been adapted to extend its suitability to materials with low ductility, as CFRP are. For instance, using a spring die [27], Friction Assisted Clinching [27,28], or softening the polymeric matrix in thermoplastic composites to increase composite toughness and formability [29–33].

These methods imply extra process steps or high complexity, which hampers their implementation in high-volume production industries. To boost MMD deployment in the automotive industry, this work presents a straightforward, cost-efficient, non-weight penalizing mechanical joining technology for metal and FRP based on a single-step punching process of the metal sheet and the uncured prepreg. The methodology can be easily implemented in automotive production lines, where punching operations are commonly used. It does not increase the weight of the part with the addition of fasteners, on the contrary, it removes part of the metallic material, making the part even lighter. In addition, the hole created in the metallic material relives stress concentrations more efficiently than the composite due to its plasticity [34]. Therefore, damage on the composite is minimized, and no additional weight is added to the structure or complexity to the joining process. Moreover, the joint does not generate any protrusion, making it suitable for completely flat applications. The proposed joining methodology is applied to bind CFRP and Al sheet alloys together.

2. Materials

A 1.5-mm-thick rolled sheets of AA5754 H111 aluminium alloy was selected for this work, as it is one of the most common non-heat-treatable aluminium alloy used in the automotive industry to produce medium strength parts thanks to its high formability and corrosion resistance. Aluminium sheets were waterjet cut perpendicular to the rolling direction. The selected FRP was a 0.65-mm-thick CFRP sheets which consisted of one layer of a 650 g/m^2 Twill 2x2 prepreg with a MTC275 toughened epoxy resin system supplied by SHD Composites.

3. Multi-material joining through punching

The mechanical joining procedure consists of laying up uncured CFRP prepreg layers on top of an aluminium sheet and punching the whole system with the CFRP facing the punch side of the set-up (Fig. 1c). A silicon paper was placed between the uncured CFRP prepreg and the punch to avoid the prepreg sticking to the punch. In addition, the aluminium surface was thoroughly cleaned with acetone using a wipe cloth to remove any surface contamination. No other aluminium surface treatment was used in this study.

By adjusting the cutting clearance and the punch stroke, the aluminium sheet is completely punched through while the carbon fibres are mostly not (Fig. 2a). Instead, these carbon fibres are pressed against the hole walls in the aluminium, generating a mechanical interlock between both materials. As joining takes place in an uncured state, delamination of the CFRP does not occur.

The mechanical interlocking joints are achieved using a punching tool (Fig. 1a) mounted on a universal testing machine (Fig. 1b). The specimens are cured afterwards by thermoforming (Fig. 2b and c). Co-curing of the composite epoxy resin on the aluminium sheet takes place and, therefore, adhesive bonding between both substrates contributes to increasing the strength of the joint.

The geometrical characteristics of the punch and the die are shown in Fig. 1c. The cutting clearance, c (eq. (1)), is defined as the ratio between the diameters of the punch (d_p) and die (d_d) gaps and the thickness of the punched material, t [35].

$$c = \frac{d_d - d_p}{2t} \cdot 100 \tag{1}$$

In the sheet metal forming industry, typical clearance values range from 5% to 20%, with 10% being the most common one [35,36]. However, higher cutting clearances have been used in this work (from 18% to 38%), to allow the carbon fibres to slide between the punch and the die without being completely cut. Another relevant punching parameter is the punch stroke (s), i.e., the penetration of the punch on the substrate being punched (Fig. 1c).

In the present work, the joints were performed at a constant punching speed of 10 mm/min by placing the CFRP at the punch side and the aluminium at the die side (Fig. 1c). The punch diameter was 10 mm, as is commonly found in many sheet metal operations [38], and the fillet radius was 0 mm (R = 0, Fig. 1c). Different combinations of process parameters (die diameter and punch stroke) were tested to determine their influence on the mechanical performance of the joint. The tested die diameters were 11.7 mm, 11.3 mm and 10.8 mm which correspond to clearance values of 18%, 29% and 38%, respectively.

Load vs stroke curves were recorded during the punching process (Fig. 4a and b). When punching a metallic sheet (Fig. 4a), three different regimes were observed [37]. The first (I) corresponds to the deformation and strain hardening of the aluminium sheet with the formation of the roll-over depth of the cut edge (Fig. 3). The second (II) corresponds to the cutting of the aluminium, generating the fracture and smooth sheared edge (Fig. 3), and the third (III) corresponds to the complete punching of the aluminium sheet.

When performing the aluminium and CFRP prepreg joint (Fig. 4b), the same punching regimes are observed, but regime II is divided into two differentiated regions: IIa and IIb. Region IIa corresponds to the cutting of the aluminium sheet. On the other hand, region IIb initiates with complete punching of the aluminium without fibre breakage and, as the punch stroke increases, carbon fibres progressively break until

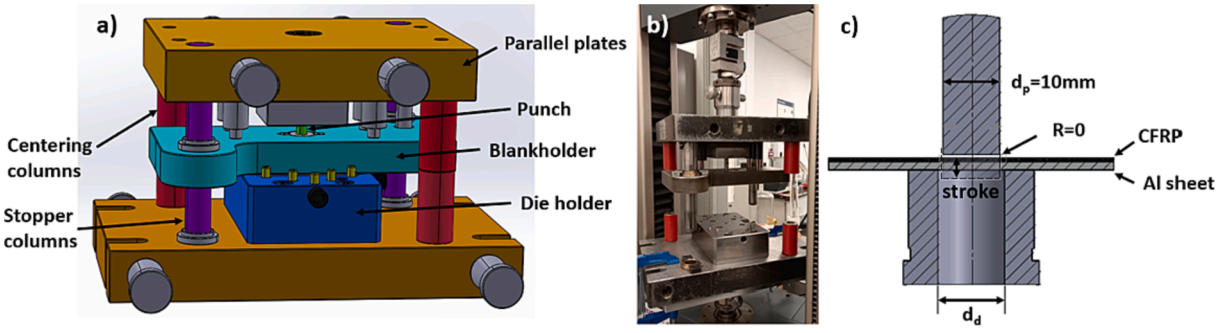

Fig. 1. A) Sketch of the punch tooling, b) corresponding experimental set-up and c) cross-section of the punch and the die. (For interpretation of the references to colour in this figure legend, the reader is referred to the web version of this article.)

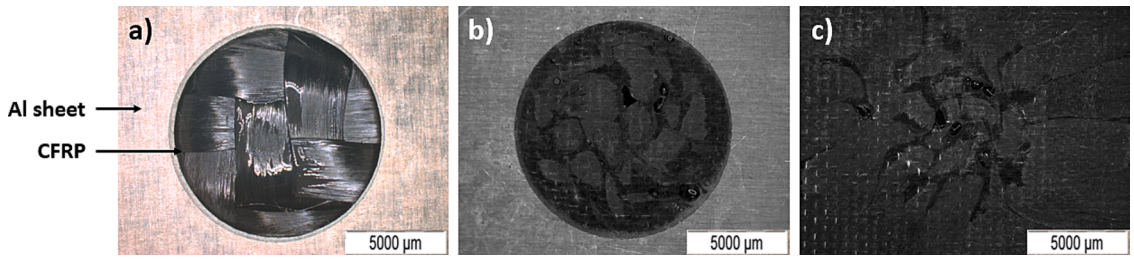

Fig. 2. a) Mechanical interlocking joint after punching and prior to curing, b) cured joint from the aluminium sheet side and c) cured joint from CFRP side. (For interpretation of the references to colour in this figure legend, the reader is referred to the web version of this article.)

Fig. 3. a) Cross-section of a punched metallic sheet with the different zones of the cut edge [39] and b) punched aluminium sheet. (For interpretation of the references to colour in this figure legend, the reader is referred to the web version of this article.)

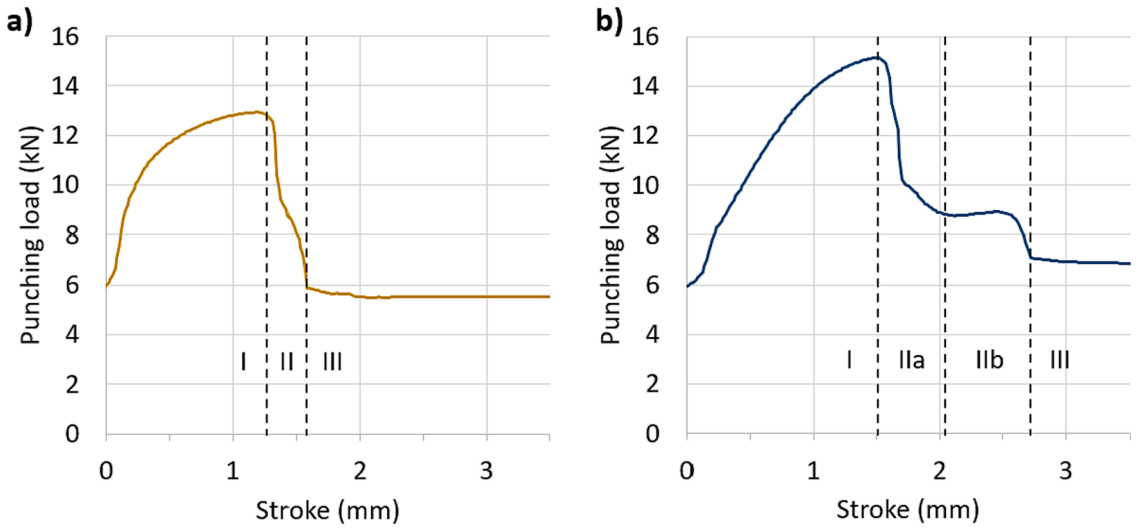

Fig. 4. Load-stroke curves when punching with $d_p = 10$ mm and $d_d = 11.7$ mm a) a 1.5-mm-thick aluminium sheet, and b) a 1.5-mm-thick aluminium sheet with CFRP prepreg. The curve starts at 6kN, which corresponds to the blankholder weight. (For interpretation of the references to colour in this figure legend, the reader is referred to the web version of this article.)

maximum fibre breakage is reached at end of regime IIb.

Thus, we selected process parameters that would punch through the aluminium sheet completely while avoiding or minimizing cutting the carbon fibres. Such conditions fall into regime IIb of the punching load vs stroke curve (Fig. 4b). Therefore, per each die diameter, a first punch operation with a long stroke was performed to obtain the complete load-stroke curve and identify the different punching regimes. Then, several joints with different punch strokes falling into regime IIb were performed.

Punching the aluminium was considered complete when the aluminium blank was removed during the process. An intermediate punching stage was also identified when the aluminium had been partially punched and the blank had to be manually removed with a screwdriver.

After punching, a rough quantification of the number of broken fibres was performed (using the naked eye) and consisted of evaluating the percentage of the joint diameter where the fibres were cut.

4. Microstructural and mechanical characterization of the joint

The cross-section of the generated joint was inspected through stereomicroscopy using an Olympus SZX10 and via epifluorescence microscopy using a Leica DMRXA microscopy with a mercury lamp. Cut edge parameters were measured using an image analysis software.

The mechanical performance of the joint was evaluated with the Single Lap Shear (SLS) test performed at room temperature using a universal testing machine at constant crosshead speed of 1 mm/min. Specimen geometry and dimensions are depicted in Fig. 5. A

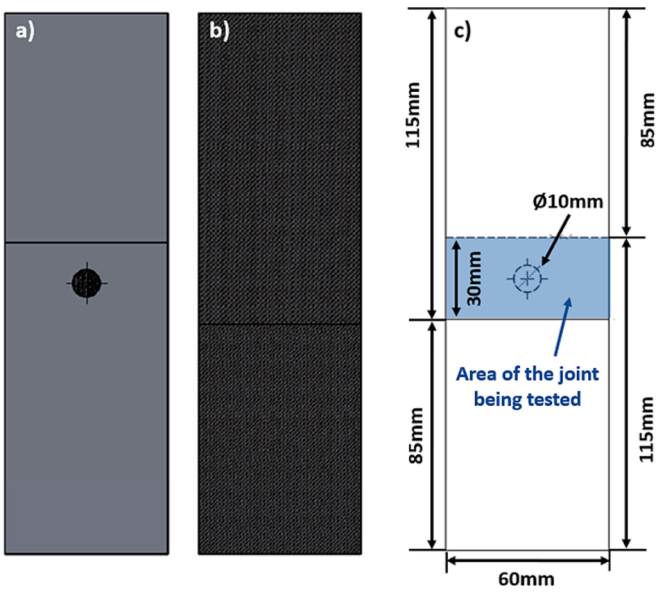

Fig. 5. Single Lap Shear specimens with one substrate being aluminium and the other being CFRP. a) Al side of the specimen, b) CFRP side of the specimen, and c) dimensioned drawing of the specimen. (For interpretation of the references to colour in this figure legend, the reader is referred to the web version of this article.)

discontinuity is present in each one of the substrates, equidistant from the specimen centre and in opposite directions for each substrate, so that the area between both discontinuities is the area of the joint being tested.

Such SLS configuration introduces peeling (mode I) and non-linear geometric effects due to the slight curvature of the specimens caused by the mismatch on the coefficient of thermal expansion between aluminium and the carbon fibres. However, this mode-mixity can also be representative of industrial applications [20] and no effort was devoted to avoiding it.

The maximum shear load, shear strength, and absorbed energy were evaluated from the load–displacement curves. Three different types of specimens with five specimens per each type, were manufactured to analyse the mechanical performance of the joint (Table 1). Reference specimens (RS) were specimens with no mechanical interlock to characterize the joint strength given by the adhesion of the epoxy resin on the aluminium substrate, mechanically interlocked specimens (MECI) were prepared with the mechanical joint developed, and manually placed specimens (MANP) were prepared to characterize the joint strength when punching only the aluminium sheet and manually placing the CFRP on top afterwards. Then, MECI specimens with different die diameters and strokes were performed to evaluate the influence of such process parameters on the mechanical performance of the joint.

Table 1
Types of specimens and process parameters.

Specimen type	Punched materials	Punching parameters		
		d_d (mm)	clearance (%)	stroke (mm)
Reference Specimens (RS)	None	–	–	–
Manually placed (MANP)	Al	11.7	57	2.3
Mechanically interlocked (MECI)	Al + CFRP	11.7	38	2.3
		11.7	38	2.4–3.0
		11.3	29	2.1–3.7
		10.8	18	2.2–3.0

5. Results

5.1. Punching load–displacement curves

Load-stroke curves (Fig. 6) show that punching the aluminium-CFRP with the CFRP prepreg (MECI) specimens involved 1 kN higher loads than aluminium punching (MANP). The punching force increased when reducing clearance; a well-known phenomenon in sheet metal punching [36,38]. In addition, the length of regime IIb decreased with the die diameter. Large fluctuations were seen in the curves obtained for the intermediate die diameter of 11.3 mm (Fig. 6b). For this die diameter, half of the curves exhibited the same behaviour than the curves obtained for the large die diameter (11.7 mm, Fig. 6a), while the other half behaved closer to the smallest die diameter (10.8 mm, Fig. 6c).

Fibre breakage scaled up with the punch stroke for all the studied die diameters. On the other hand, punch strokes that were too short led to incomplete sheet punching. Small die diameters led to complete sheet punching, while large die diameters led to partial sheet punching. In this latter case, the aluminium blank had to be removed manually using a screwdriver.

5.2. Joint geometry

The top view of MECI and MANP specimens performed with the same punching parameters (Fig. 7) shows that MANP have a burr, while MECI do not. The MANP burrs are flattened during the curing process and these specimens show a dry region in the CFRP side of the joint.

The cross-section of the joints was inspected with stereomicroscopy (Fig. 8a) and epifluorescence (Fig. 8b). The Twill 2x2 weave from the CFRP can be clearly observed in both images. Epoxy resin fluorescence generates a clearer contrast between the fibres (black) and the epoxy resin (yellow). This indicates that the carbon fibres are pressed against the roll-over depth of the aluminium cut edge, while the area of the hole in contact with the fracture depth is resin rich. The carbon fibres have filled the rest of the aluminium hole.

The cross-sections of punched aluminium sheets, MANP, and MECI specimens were also inspected with stereomicroscopy (Fig. 9). The morphology of the Al sheet cut edge was modified with the incorporation of the CFRP in the punching process. Punched aluminium sheets without CFRP present four different regions at the cut edge: roll-over depth, smooth-sheared depth, fracture depth and burr (Fig. 9). The same four regions can be observed in MANP specimens, since only the aluminium sheet is punched and the CFRP prepreg is placed afterwards. However, the sheet burr in the MANP specimens is flattened out due to curing pressure. On the other hand, when incorporating the carbon fibre prepreg in the punching step (MECI specimens), the burr disappears and the smooth-sheared and fracture depth are fused into a single region. Therefore, only the roll-over depth and fracture depth are present in the cut edge, regardless of the clearance.

In addition, the carbon fibres in the MANP specimens lay only at the top of the aluminium hole, while the rest of the hole is filled with resin. On the other hand, on MECI specimens, the carbon fibres reach the bottom of the aluminium hole (Fig. 9).

The cross-section of MECI specimens manufactured with three different die diameters and four different punch strokes can be observed in Fig. 10. Roll-over depth increases with increasing clearance when punching only aluminium sheets thanks to the increased lever arm, as commonly observed in sheet metal punching [37]. However, when aluminium with carbon fibre prepreg is punched, the opposite trend is observed, and the roll-over depth increases when the cutting clearance decreases. Cut fibre is observed in specimens with higher stroke (3.3 mm) regardless of the clearance. When decreasing the stroke, the number of broken fibres decreases.

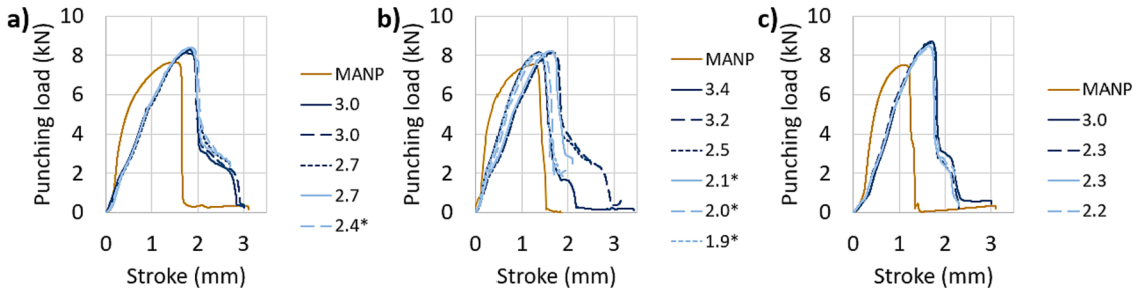

Fig. 6. Load vs punch stroke curves for MANP specimens (yellow) and MECI specimens (rest) with different punch strokes (specified in the legend). The following die diameters were used: a) 11.7 mm, b) 11.3 mm, and c) 10.8 mm. The asterisk marks uncomplete punching of the aluminium. (For interpretation of the references to colour in this figure legend, the reader is referred to the web version of this article.)

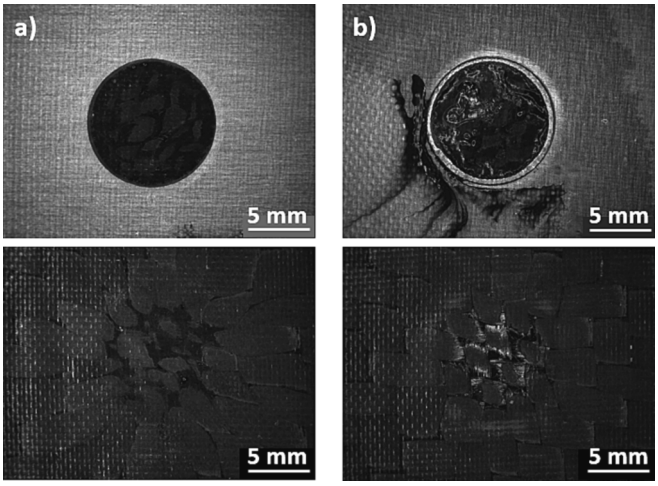

Fig. 7. Mechanical interlocks performed with d_d = 11.3 mm and stroke of 3.3 mm a) MECI and b) MANP specimens.

5.3. Single lap shear tests

Load-displacement curves obtained for the SLS tests of the RS, MECI and MANP specimens are shown in Fig. 11. Shear strength vs weight performance of the joint improved 41% and the absorbed energy 94% for MECI specimens with respect to RS. Average maximum sheal load and absorbed energy for the RS was 5.6 kN and 3.3 J respectively, and increased to 7.9 kN and 6.4 J for MECI specimens. For the MANP specimens, however, the increase in the maximum shear load was 34%, obtaining an average of 7.6 kN, and absorbed energy was improved by 57%, obtaining 5.2 J (Fig. 12).

All RS specimens showed adhesive failure between the CFRP and the aluminium substrate (Fig. 13a). MECI specimens failed by complete pull-out of the CFRP bulge from the aluminium hole (Fig. 13b). However, MANP specimens failed in the resin-fibre interface of the composite material and only carbon fibres were pulled out of the aluminium hole, while a resin layer remained at the bottom of the hole (Fig. 13c). Catastrophic failure occurred for both RS and MANP, whereas a more progressive failure was observed for the MECI specimens, with several small drops before the load peak and a non-zero load queue after the big load drop (Fig. 11b).

SLS Load-displacement curves of MECI specimens using different die diameters and strokes were also obtained (Fig. 14). MECI specimens obtained with the 11.3 mm die diameter (Fig. 14c) showed some degree of fluctuation in the elastic phase at different strokes. Other than that, no clear effect of varying the punch stroke was observed on the mechanical properties of the joint per each given die diameter.

However, the average maximum shear load obtained per each die diameter increased slightly with decreasing die diameter (Fig. 15). Reference specimens (RS) with no mechanical interlock achieved a maximum shear load of 5.6 kN, while the maximum shear load of mechanical interlocked samples ranged from 8.5 kN for the biggest die diameter (d_d = 11.7 mm) to 8.6 kN for the smallest die diameter (d_d = 10,8 mm). Therefore, the mechanical interlock improved the shear strength per weight of the joint for the Twill material by between 51% and 57%. Regarding the energy absorbed before failure, the highest value was obtained for intermediate die diameters (d_d = 11.3 mm). The absorbed energy increased with the mechanical interlock, from 3.3 J for the RS samples to 10.1 J for the MI samples with a 11.3 mm die diameter. Hence, absorbed energy was improved by the mechanical interlock

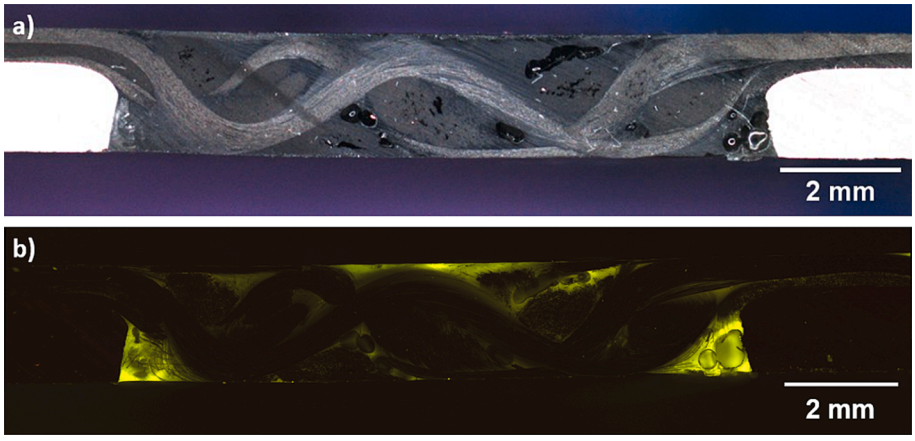

Fig. 8. Cross-section of the joint generated with d_d = 11.3 mm and 3.3 mm stroke inspected using a) stereomicroscope and b) epifluorescence. (For interpretation of the references to colour in this figure legend, the reader is referred to the web version of this article.)

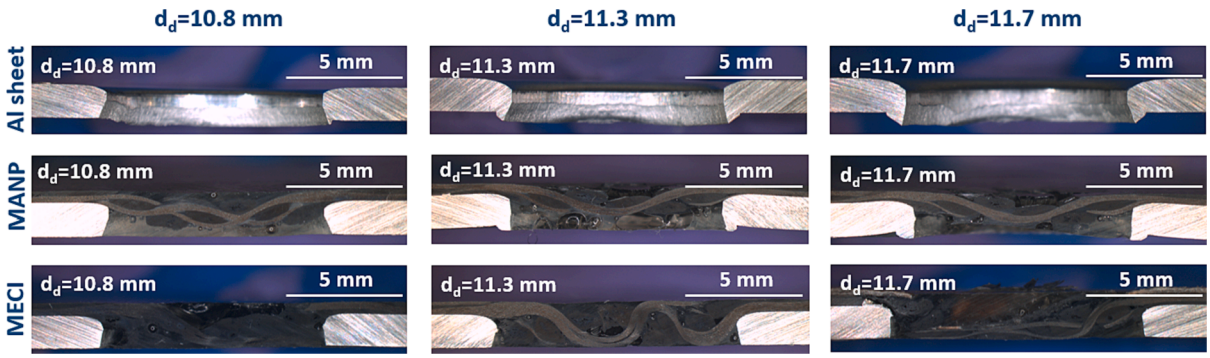

Fig. 9. Cross-section of aluminium sheets, MANP and MECI specimens generated with different die diameters. (For interpretation of the references to colour in this figure legend, the reader is referred to the web version of this article.)

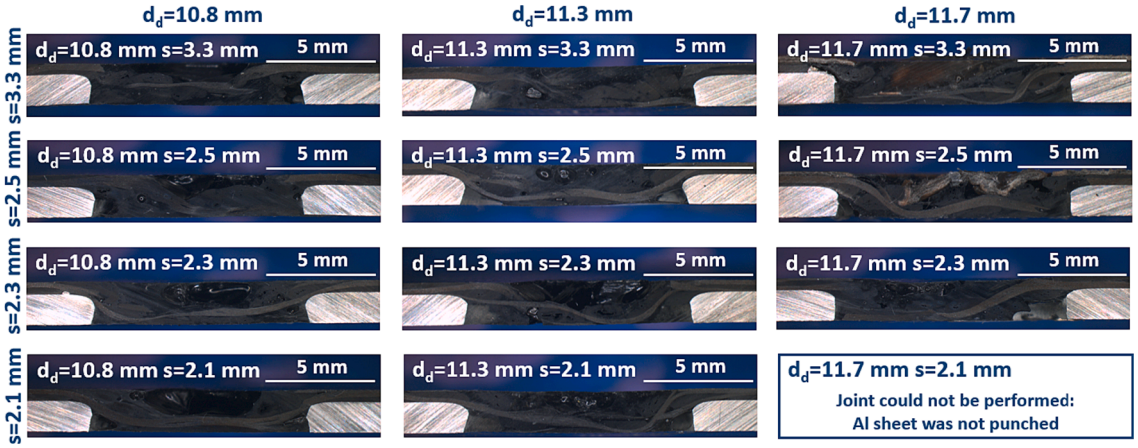

Fig. 10. Cross-section of MECI specimens for different die diameters (d_d = 10.8 mm, d_d = 11.3 mm and d_d11.7 mm) and different punch strokes (s = 3.3 mm, s = 2.5 mm, s = 2.3 mm and s = 2.1 mm). (For interpretation of the references to colour in this figure legend, the reader is referred to the web version of this article.)

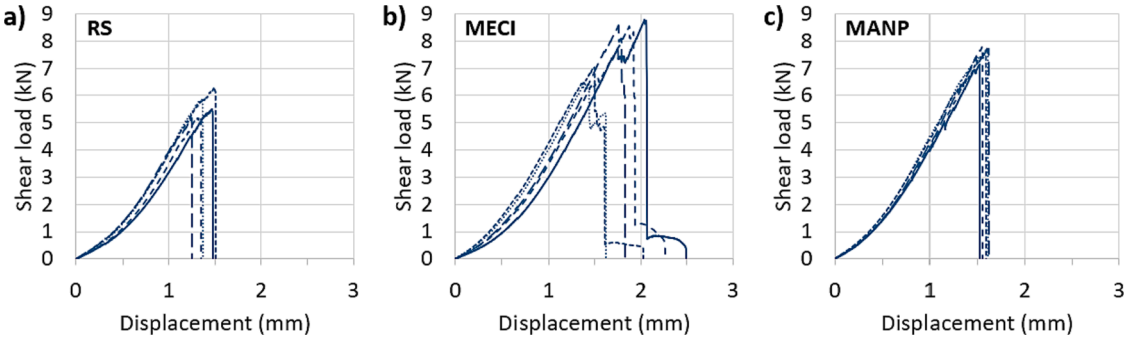

Fig. 11. Load-displacement curves obtained in the SLS test for a) reference samples (RS), b) mechanically interlocked samples (MECI) and c) manually placed samples (MANP). (For interpretation of the references to colour in this figure legend, the reader is referred to the web version of this article.)

between 176% and 205%.

6. Discussion

The present work describes a new type of joining methodology which is counterintuitive, since the aluminium sheet (in contact with the die) can be punched without completely cutting the carbon fibres (in contact with the punch). This is possible because the punch penetrates the material slightly before the actual cutting, thus compressing the aluminium surface near the punch and inducing strain hardening on the material. Therefore, the resistance of the material to penetration rises and material fracture does not start on the edge close to the punch, but rather occurs on the soft area close to the die, which is not hardened [39].

Since punching is performed with the uncured prepreg, the polymeric resin is in a viscous flow state, and therefore delamination and CFRP tear around the joining area are reduced. When curing, the epoxy resin flows inside the aluminium hole and fills it up. Consequently, there is a resin rich region near the fracture depth of the aluminium cut edge (Fig. 8) and the fibres are less compacted inside the aluminium hole than on the rest of the specimen.

Regarding the process window, the punch strokes that allow the joint to be generated are those from within punching regime IIb, where the aluminium is completely punched but the CFRP is not. The extension of this regime IIb decreases with the cutting clearance and this decrease is

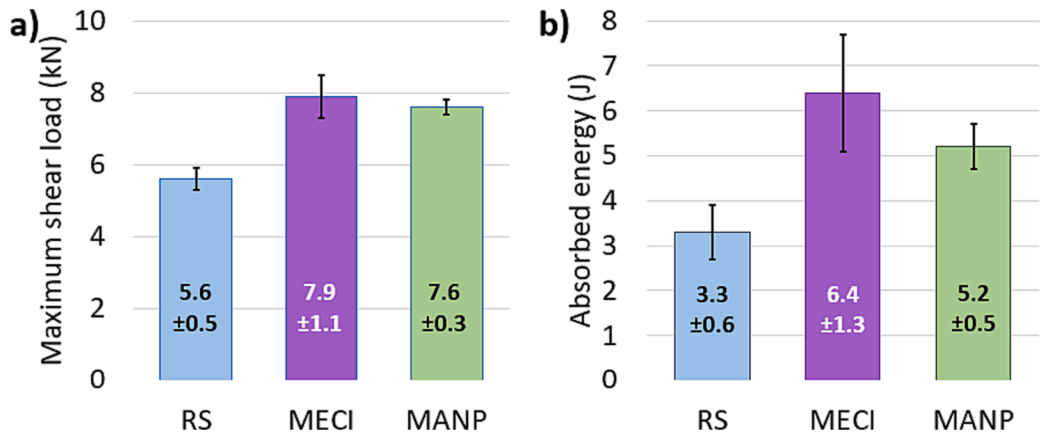

Fig. 12. SLS average results with standard deviation for RS, MECI and MANP specimens regarding a) maximum shear load and b) absorbed energy. (For interpretation of the references to colour in this figure legend, the reader is referred to the web version of this article.)

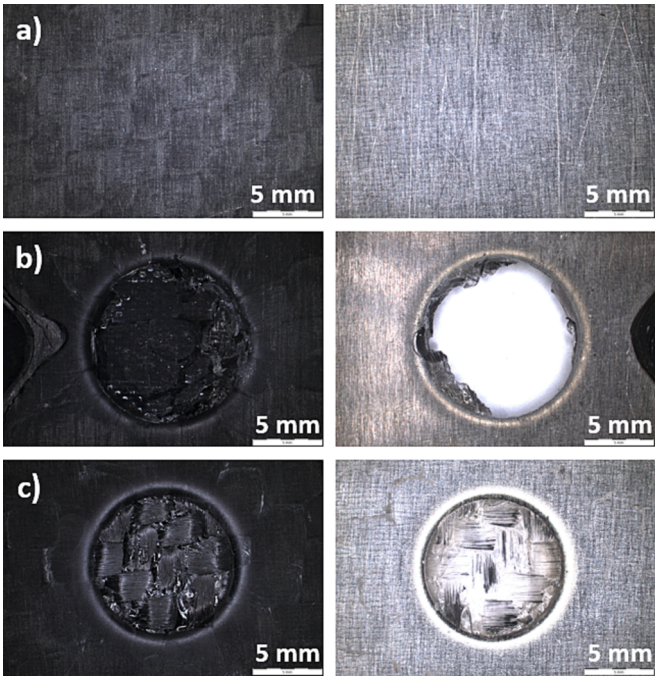

Fig. 13. Joint region of SLS specimens after failure a) RS specimens, b) MECI specimens and c) MANP specimens. (For interpretation of the references to colour in this figure legend, the reader is referred to the web version of this article.)

accentuated once we reach clearance values smaller than the one where the gap between the punch and the die equals the CFRP thickness (0.65 mm). This is because carbon fibres are then squeezed between the punch and the die, which impedes fibres sliding through the aluminium hole without being cut. Consequently, carbon fibres are therefore cut at shorter punch strokes.

Additionally, when punching an aluminium sheet together with a CFRP prepreg (MECI specimens), the cut edge geometry is changed with respect to when only punching aluminium sheets (MANP specimens). The smooth-sheared depth and the burr vanish due to the presence of the carbon fibres (Fig. 9). These fibres fill the gap between the punch and the die during the punching process, reducing the effective clearance and leaving no free space for burr formation. In addition, burnishing does not take place and, therefore, the smooth-sheared depth cannot be formed. Furthermore, in MECI specimens the roll-over depth increases when the clearance decreases, thus following the opposite trend showed when punching only the aluminium sheet (Fig. 10). This was again attributed to smaller clearances leading to higher carbon fibre tension and aluminium compression, resulting in larger deformation and roll-over depths.

Both MECI and MANP specimens increased the mechanical performance of the co-cured RS joints in terms of shear strength and absorbed energy. However, the mechanical performance in the MECI specimens is higher than in the MANP ones, especially when it comes to the absorbed energy before failure. This can be attributed to the different failure mode given by the different disposition of the carbon fibres through-the-hole-thickness. When punching only the aluminium and placing the prepreg afterwards (MANP specimens), the carbon fibres remain on the upper part of the aluminium hole, and only resin fills the bottom of the hole (Fig. 9). Because of this, failure in MANP specimens when subjected to an SLS test occurred in the resin-fibre interface of the composite bulge (Fig. 13c), with loss of adhesion between the fibres and the epoxy matrix. On the other hand, when punching both materials together (MECI specimens), the punch pushes the CFRP all the way down through the aluminium hole. Because of this, MECI specimens fail by CFRP bulge unbuttoning (Fig. 13b), leading to less catastrophic failure and a higher shear strength and absorbed energy than MANP specimens. Another contribution to the higher mechanical properties of these specimens can be the strain hardening caused in the hole surroundings, which is due to the aluminium compression caused by the tension introduced into the carbon fibres when punching. This can also explain why in MECI specimens, the shear strength increases slightly when reducing the clearance, since the lower the clearance, the higher the tension on the carbon fibres and, thus, the higher the strain hardening in the vicinity of the hole.

Evaluation of the effect of clearance and punch stroke on processability and mechanical performance of the joint showed that the punch stroke had no significant effect on the mechanical performance, but that long punch strokes led to high percentages of broken fibres, whereas short punch strokes were not enough to completely punch the aluminium. Moreover, the lower the clearance, the shorter the stroke needed to perforate the aluminium due to the increased shear stress at the cut edge. Low clearances also led to completely punching the aluminium without further process steps. Consequently, small clearances are recommended to achieve higher mechanical performance while simplifying the process and lowering cycle time.

It must be pointed out that the developed joining process creates intimate surface contact between the aluminium and the carbon fibres. Since both materials are electrically conductive and have a large difference in their electrochemical potentials, this arrangement is susceptible to galvanic corrosion in the presence of an electrolyte . Potential mitigation concepts for this would be to add a glass fiber layer in

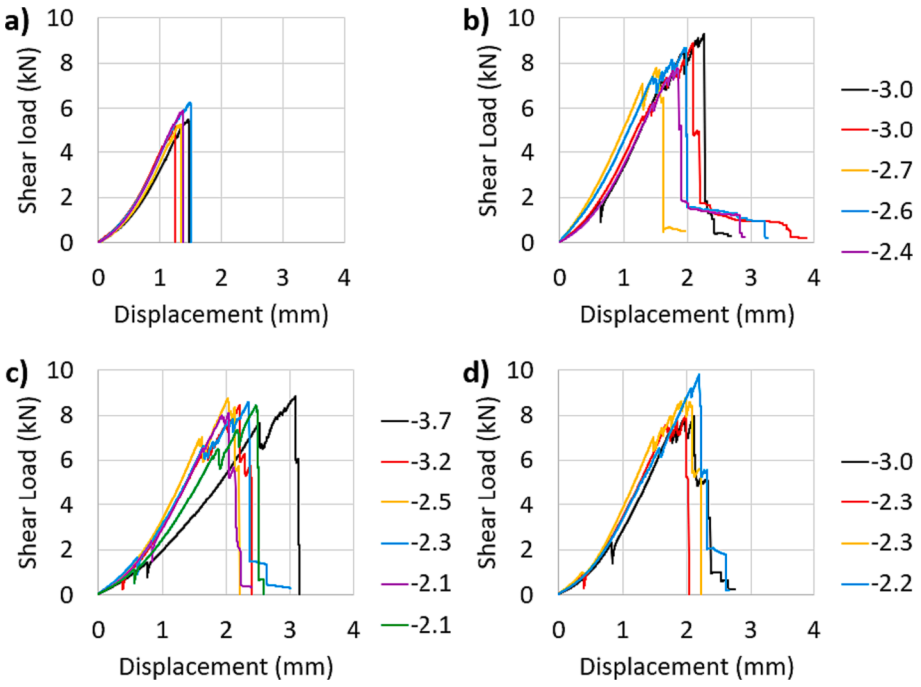

Fig. 14. SLS load–displacement curves for MECI specimens generated with different punch strokes (specified in the legend) and the following die diameters a) none (RS), b) $d_d = 11.7$ mm, c) $d_d = 11.3$ mm and d) $d_d = 10.8$ mm. (For interpretation of the references to colour in this figure legend, the reader is referred to the web version of this article.)

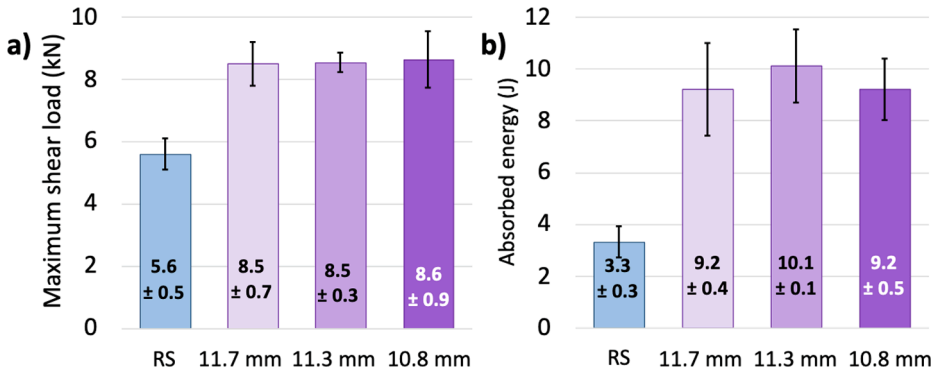

Fig. 15. SLS average results with standard deviation for RS and MECI specimens manufactured with 11.7 mm, 11.3 mm and 10.8 mm die diameters for a) maximum shear load and b) absorbed energy. (For interpretation of the references to colour in this figure legend, the reader is referred to the web version of this article.)

between the carbon fiber and the aluminium, to add a resin rich layer or an adhesive layer between both materials, or to use a different metal which is closer to carbon in the galvanic series, such as stainless steel or titanium.

The mechanical behaviour of the developed joint was compared to other similar joining methodologies for composites and sheet metals found in the open literature (Fig. 16). This comparison needs to be taken as qualitative, since the metallic sheet and composite material are different for every study. As each reference uses a different specimen geometry, the shear strength (σ_s) was calculated according to eq. (2), where F_s is the maximum shear load and A_j is the area of the joint subjected to shear load, corresponding to the overlapped area between both substrates.

$$\sigma_s = \frac{F_s}{A_j} \tag{2}$$

It can be seen that the developed MECI joints perform in the same range than the hole clinching technology, which implies a complicated process and long processing times because it requires a hole to be drilled in the composite and then aligning the hole with the clinching device. It can also be seen that the joint strengths obtained with the MECI joints were superior than some of the mechanical clinching modificacions, even when comparing to mechanical clinching of thermoplastic composites, where there is also adhesive bonding in addition to mechanical interlocking. Therefore, the interlocking procedure presented in this work can be postulated as an interesting alternative to join dissimilar materials in engineering applications.

7. Conclusions

A new mechanical joining methodology for a metal sheet and an FRP based on a single-step punching process was developed. The technology is not only simple, cost-efficient, and non-weight penalizing, it also avoids damage in the composite material and does not add complexity to the joining process.

Such mechanical interlocking joint improves the shear strength of the co-cured joint between 41% and 57% and the absorbed energy between 94% and 205% for the studied materials.

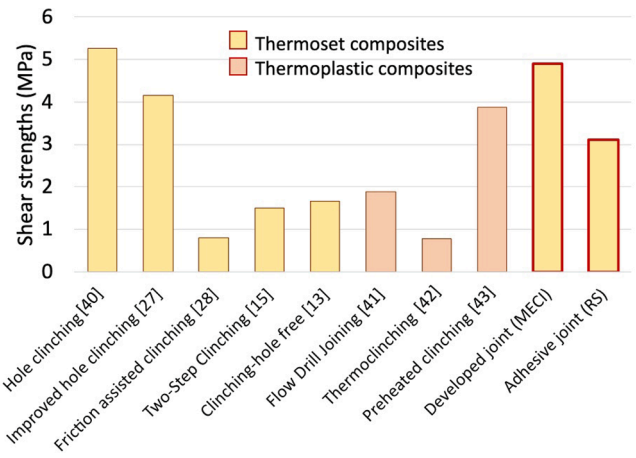

Fig. 16. Shear strengths calculated from the maximum shear loads and the joint area for different clinching technologies. The references where the data was extracted from are given after each technology [13,15,27,28,30,40–43]. The two columns in the right marked with thicker contour stand for the joint developed in this work (MECI) and the adhesive joint used as a reference (RS). (For interpretation of the references to colour in this figure legend, the reader is referred to the web version of this article.)

The effect of the most relevant process parameters (cutting clearance and punch stroke) was evaluated. The shear strength increased when decreasing the clearance between the punch and the die, while the punch stroke had no clear influence on the mechanical performance of the joint. Process-wise, small clearances are recommended to achieve higher mechanical performance, simplify the process, and lower the cycle time.

Finally, the mechanical performance of the joint was found to be within the same range as other mechanical metal-composite joining methodologies such as clinching.

CRediT authorship contribution statement

Núria Latorre: Conceptualization, Methodology, Validation, Formal analysis, Investigation, Resources, Data curation, Writing – original draft, Visualization, Project administration. **Daniel Casellas:** Conceptualization, Methodology, Writing – review & editing, Supervision, Funding acquisition. **Josep Costa:** Conceptualization, Methodology, Writing – review & editing, Supervision.

Declaration of Competing Interest

The authors declare the following financial interests/personal relationships which may be considered as potential competing interests: Daniel Casellas reports financial support was provided by Government of Catalonia. Nuria Latorre reports equipment, drugs, or supplies was provided by Aludium Alicante. Nuria Latorre, Daniel Casellas reports a relationship with RISE Research Institutes of Sweden AB that includes: non-financial support. Nuria Latorre, Daniel Casellas, Josep Costa has patent #EP22383176.9 pending to Fundació Eurecat and Universitat de Girona. Co-author Josep Costa is currently on the editorial board of the journal Composites Part A.

Data availability

Data will be made available on request.

Acknowledgments

Núria Latorre is a fellow of Eurecat's "Vicente López" PhD grant program. This work was financially supported by the Catalan Government through the funding grant ACCIÓ-Eurecat (Project Flagship-Intelligent).

Open Access funding provided thanks to the CRUE-CSIC agreement with Elsevier.

The authors would like to thank Aludium for providing the AA5754 H111 aluminium sheets. Gratitude is also extended to Daniel Berglund and Yvonne Aitomäki from the Research Institute of Sweden (RISE) and to David Frómeta from Eurecat for fruitful discussions, and to Toni Lara, Sergi Parareda and Genís Arderiu from Eurecat for the technical assistance in punching and mechanical testing.

References

[1] Fleischer J, Nieschlag J. Introduction to CFRP-metal hybrids for lightweight structures. Prod Eng 2018;12(2):109–11. https://doi.org/10.1007/s11740-018-0825-0.
[2] Lim TS, Kim BC, Lee DG. Fatigue characteristics of the bolted joints for unidirectional composite laminates. Compos Struct 2006;72(1):58–68. https://doi.org/10.1016/j.compstruct.2004.10.013.
[3] Pramanik A, Basak AK, Dong Y, Sarker PK, Uddin MS, Littlefair G, et al. Joining of carbon fibre reinforced polymer (CFRP) composites and aluminium alloys – A review. Compos A Appl Sci Manuf 2017;101:1–29. https://doi.org/10.1016/j.compositesa.2017.06.007.
[4] Thoppul SD, Finegan J, Gibson RF. Mechanics of mechanically fastened joints in polymer-matrix composite structures - A review. Compos Sci Technol 2009;69(3–4):301–29. https://doi.org/10.1016/j.compscitech.2008.09.037.
[5] Ouyang Y, Chen C. Research advances in the mechanical joining process for fiber reinforced plastic composites. Compos Struct 2022;296(March):115906. https://doi.org/10.1016/j.compstruct.2022.115906.
[6] Galińska A. Mechanical joining of fibre reinforced polymer composites to metals—a review. Part I: Bolted joining. Polymers (Basel) 2020;12(10):1–48. https://doi.org/10.3390/polym12102252.
[7] Olmedo Á, Santiuste C. On the prediction of bolted single-lap composite joints. Compos Struct 2012;94(6):2110–7. https://doi.org/10.1016/j.compstruct.2012.01.016.
[8] Di Franco G, Fratini L, Pasta A. Analysis of the mechanical performance of hybrid (SPR/bonded) single-lap joints between CFRP panels and aluminum blanks. Int J Adhes Adhes 2013;41:24–32. https://doi.org/10.1016/j.ijadhadh.2012.10.008.
[9] Zhang J, Yang S. Self-piercing riveting of aluminum alloy and thermoplastic composites. J Compos Mater 2015;49(12):1493–502. https://doi.org/10.1177/0021998314535456.
[10] Gay A, Lefebvre F, Bergamo S, Valiorgue F, Chalandon P, Michel P, et al. Fatigue performance of a self-piercing rivet joint between aluminum and glass fiber reinforced thermoplastic composite. Int J Fatigue 2016;83:127–34. https://doi.org/10.1016/j.ijfatigue.2015.10.004.
[11] Wang J, Zhang G, Zheng X, Li J, Li X, Zhu W, et al. A self-piercing riveting method for joining of continuous carbon fiber reinforced composite and aluminum alloy sheets. Compos Struct 2021;259:113219. https://doi.org/10.1016/j.compstruct.2020.113219.
[12] Lambiase F. Mechanical behaviour of polymer-metal hybrid joints produced by clinching using different tools. Mater Des 2015;87:606–18. https://doi.org/10.1016/j.matdes.2015.08.037.
[13] Lambiase F, Ko DC. Feasibility of mechanical clinching for joining aluminum AA6082-T6 and Carbon Fiber Reinforced Polymer sheets. Mater Des 2016;107:341–52. https://doi.org/10.1016/j.matdes.2016.06.061.
[14] Lambiase F, Durante M, Ilio AD. Fast joining of aluminum sheets with Glass Fiber Reinforced Polymer (GFRP) by mechanical clinching. J Mater Process Technol 2016;236:241–51.
[15] Lambiase F, Ko DC. Two-steps clinching of aluminum and Carbon Fiber Reinforced Polymer sheets. Compos Struct 2017;164:180–8. https://doi.org/10.1016/j.compstruct.2016.12.072.
[16] Caminero MA, Lopez-Pedrosa M, Pinna C, Soutis C. Damage monitoring and analysis of composite laminates with an open hole and adhesively bonded repairs using digital image correlation. Compos B Eng 2013;53:76–91. https://doi.org/10.1016/j.compositesb.2013.04.050.
[17] Mishra R, Malik J, Singh I, Davim JP. Neural network approach for estimating the residual tensile strength after drilling in uni-directional glass fiber reinforced plastic laminates. Mater Des 2010;31(6):2790–5. https://doi.org/10.1016/j.matdes.2010.01.011.
[18] Ucsnik S, Scheerer M, Zaremba S, Pahr DH. Experimental investigation of a novel hybrid metal-composite joining technology. Compos A Appl Sci Manuf 2010;41(3):369–74. https://doi.org/10.1016/j.compositesa.2009.11.003.
[19] Graham DP, Rezai A, Baker D, Smith PA, Watts JF. The development and scalability of a high strength, damage tolerant, hybrid joining scheme for composite-metal structures. Compos A Appl Sci Manuf 2014;64:11–24. https://doi.org/10.1016/j.compositesa.2014.04.018.
[20] Parkes PN, Butler R, Meyer J, de Oliveira A. Static strength of metal-composite joints with penetrative reinforcement. Compos Struct 2014;118(1):250–6. https://doi.org/10.1016/j.compstruct.2014.07.019.
[21] Nguyen ATT, Brandt M, Feih S, Orifici AC. Pin pull-out behaviour for hybrid metal-composite joints with integrated reinforcements. Compos Struct 2016;155:160–72. https://doi.org/10.1016/j.compstruct.2016.07.047.

[22] Nguyen ATT, Amarasinghe CK, Brandt M, Feih S, Orifici AC. Loading, support and geometry effects for pin-reinforced hybrid metal-composite joints. Compos A Appl Sci Manuf 2017;98:192–206. https://doi.org/10.1016/j.compositesa.2017.03.019.
[23] Möller F, Thomy C, Vollertsen F, Schiebel P, Hoffmeister C, Herrmann AS. Novel method for joining CFRP to aluminium. Phys Procedia 2010;5(PART 2):37–45. https://doi.org/10.1016/j.phpro.2010.08.027.
[24] Galińska A, Galiński C. Mechanical joining of fibre reinforced polymer composites to metals-A review. Part II: Riveting, clinching, non-adhesive form-locked joints, pin and loop joining. Polymers (Basel) 2020;12(8):pp. https://doi.org/10.3390/POLYM12081681.
[25] Camanho PP, Tavares CML, De Oliveira R, Marques AT, Ferreira AJM. Increasing the efficiency of composite single-shear lap joints using bonded inserts. Compos B Eng 2005;36(5):372–83. https://doi.org/10.1016/j.compositesb.2005.01.007.
[26] Li R, Kelly D, Crosky A. Strength improvement by fibre steering around a pin loaded hole. Compos Struct 2002;57(1–4):377–83. https://doi.org/10.1016/S0263-8223(02)00105-8.
[27] Lee CJ, Kim BM, Kang BS, Song WJ, Ko DC. Improvement of joinability in a hole clinching process with aluminum alloy and carbon fiber reinforced plastic using a spring die. Compos Struct 2017;173:58–69. https://doi.org/10.1016/j.compstruct.2017.04.010.
[28] Lambiase F, Paoletti A. Friction-assisted clinching of Aluminum and CFRP sheets. J Manuf Process 2018;31:812–22. https://doi.org/10.1016/j.jmapro.2018.01.014.
[29] Lambiase F, Paoletti A, Di Ilio A. Advances in Mechanical Clinching: Employment of a Rotating Tool. Procedia Eng 2017;183:200–5. https://doi.org/10.1016/j.proeng.2017.04.021.
[30] Gude M, Hufenbach W, Kupfer R, Freund A, Vogel C. Development of novel form-locked joints for textile reinforced thermoplastics and metallic components. J Mater Process Technol 2015;216:140–5. https://doi.org/10.1016/j.jmatprotec.2014.09.007.
[31] Lin PC, Fang JC, Lin JW, Van Tran X, Ching YC. Preheated (heat-assisted) clinching process for Al/CFRP cross-tension specimens. Materials (Basel) 2020;13(18):pp. https://doi.org/10.3390/ma13184170.
[32] Gröger B, Troschitz J, Vorderbrüggen J, Vogel C, Kupfer R, Meschut G, et al. Clinching of thermoplastic composites and metals—a comparison of three novel joining technologies. Materials (Basel) 2021;14(9):2286.
[33] Troschitz J, Kupfer R, Gude M. Process-integrated embedding of metal inserts in continuous fibre reinforced thermoplastics. Procedia CIRP 2020;85:83–8. https://doi.org/10.1016/j.procir.2019.09.039.
[34] Gamdani F, Boukhili R, Vadean A. Tensile strength of open-hole, pin-loaded and multi-bolted single-lap joints in woven composite plates. Mater Des 2015;88:702–12. https://doi.org/10.1016/j.matdes.2015.09.008.
[35] Frómeta D, Lara A, Parareda S, Casellas D. Evaluation of edge formability in high strength sheets through a fracture mechanics approach. AIP Conference Proceedings 2019;2113(July). https://doi.org/10.1063/1.5112704.
[36] Lange K. Handbook of Metal Forming. J Appl Metalwork 1986;4(2):188. https://doi.org/10.1007/BF02834383.
[37] Nothhaft K, Suh J, Golle M, Picas I, Casellas D, Volk W. Shear cutting of press hardened steel: Influence of punch chamfer on process forces, tool stresses and sheared edge qualities. Prod Eng 2012;6(4–5):413–20. https://doi.org/10.1007/s11740-012-0404-8.
[38] Kadarno P, Mori KI, Abe Y, Abe T. Punching process including thickening of hole edge for improvement of fatigue strength of ultra-high strength steel sheet. Manuf Rev 2016;1(March):2014. https://doi.org/10.1051/mfreview/2014003.
[39] Tekiner Z, Nalbant M, Gürün H. An experimental study for the effect of different clearances on burr, smooth-sheared and blanking force on aluminium sheet metal. Mater Des 2006;27(10):1134–8. https://doi.org/10.1016/j.matdes.2005.03.013.
[40] Lee CJ, Lee SH, Lee JM, Kim BH, Kim BM, Ko DC. Design of hole-clinching process for joining CFRP and aluminum alloy sheet. Int J Precis Eng Manuf 2014;15(6):1151–7. https://doi.org/10.1007/s12541-014-0450-6.
[41] Seidlitz H, Ulke-Winter L, Kroll L. New Joining Technology for Optimized Metal/Composite Assemblies. J Eng (United Kingdom) 2014;2014(September):2014. https://doi.org/10.1155/2014/958501.
[42] Vorderbrüggen J, Gröger B, Kupfer R, Hoog A, Gude M, Meschut G. Phenomena of forming and failure in joining hybrid structures - Experimental and numerical studies of clinching thermoplastic composites and metal. AIP Conference Proceedings 2019;2113:1–7. https://doi.org/10.1063/1.5112580.
[43] Lin PC, Lin JW, Li GX. Clinching process for aluminum alloy and carbon fiber-reinforced thermoplastic sheets. Int J Adv Manuf Technol 2018;97(1–4):529–41. https://doi.org/10.1007/s00170-018-1960-7.